Turkish Journal of Electrical Engineering & Computer Sciences

http://journals.tubitak.gov.tr/elektrik/

Research Article

Turk J Elec Eng & Comp Sci
(2019) 27: 4689 – 4701

doi:10.3906/elk-1901-214

Dynamic radar cross-section characteristic analysis of wind turbine based on scaled model experimental

Bo TANG, Hao CHEN*, Li HUANG, Fating YUAN, Peng FENG
College of Electrical Engineering & New Energy, China Three Gorges University, Yichang, China

Received: 29.01.2019 • **Accepted/Published Online:** 29.08.2019 • **Final Version:** 26.11.2019

Abstract: Accurately acquiring and analyzing the dynamic radar cross-section (RCS) of wind turbine have a great significance to solve the reradiation interference between wind farms and radar stations. Since the results of high-frequency approximation algorithm are only applicable to the qualitative analysis of electromagnetic scattering, it is almost impossible to accurately acquire the dynamic RCS of wind turbine in actual engineering cases. To this end, we proposed to acquire the dynamic RCS of wind turbine based on the scaled model experimental measurement in a large anechoic chamber. The key techniques of setting up the scaled model as well as the experimental platform were described based on the principle of electromagnetic similarity. The accuracy of experimental result is verified by the comparison with numerical calculation and full-sized experiment reported in literature. By using the control variable method, we were able to measure and analyze the amplitude and phase variation of dynamic RCS with frequency, azimuth, and rotational speed, and achieved the transformation of RCS data into engineering practice. This not only lays a foundation for solving the reradiation interference between wind farms and radar stations, but also provides data support for subsequent theoretical research.

Key words: Reradiation interference, wind turbine scaled model, dynamic radar cross-section, experimental measurement

1. Introduction

Large array-arranged wind turbines would induce serious reradiation interference to nearby radar stations, due to the site conflict between wind farm and radar stations [1–3]. According to the basic radar equation, a way for suppressing this interference by reducing the radar cross-section (RCS) on wind turbine side was proposed [4,5]. In addition, the rotational motion of the wind turbine blades will cause the RCS to change with time. Therefore, this calls for the accurate acquirement and characteristic analysis of dynamic RCS of wind turbine, which would be difficult using the existing measures.

On the one hand, recent studies on acquiring dynamic RCS are mainly based on either numerical calculation or experimental measurements. A common numerical calculation method is to adopt the high-frequency approximation algorithm to solve the static RCS for different stances of blades using the quasistatic method, and then reconstructs the time series of dynamic RCS [5,6]. While having a large amount of computation, this method can only obtain RCS not accurate enough, so it is normally used for qualitative analysis.

On the other hand, most of the experimental measurements were carried out on scaled models since the accuracy of full-sized experiment are greatly affected by environmental factors [7]. Lots of reported scaled model

*Correspondence: 601225027@qq.com

experiments were only able to measure static RCS. For example, Bornkessel et al. established a wind turbine scaled model of 1:73 and they measured and analyzed the static RCS of the scaled model under different parameters such as yaw angle, blade position, and pitch [8]. However, the acquired static RCS is far from satisfying the analysis of dynamic scatting characteristic of wind turbine in actual engineering, experiments to acquire dynamic RCS is necessary. Ballesteros et al. measured the dynamic RCS of an iron blade model under normal and fault conditions to analyze the fault type of wind turbine blades. Unfortunately, the shape of blades were very casual, which made the RCS data unavailable [9]. La et al. made a 1:10 iron blade scaled model and measured the static RCS of blade at different stances, and then similar to the quasistatic method, reconstructed the dynamic RCS. However, further application of this method is limited since accuracy of the measurement is related to not only the rotation step of blade, but also the material of blade [10]. Zhang et al., aiming at the measurement of radar echo of wind turbine, used resin to produce a 1:100 scaled model of wind turbine controlled by clicker [11]. However, since this scaled model was covered with aluminum foil to enhance the amplitude of RCS, its RCS data were only useful in qualitative analysis.

In order to improve the accuracy of dynamic RCS measurement of wind turbine, we produced a wind turbine scaled model with full consideration of material properties, and achieved accurate measurement of dynamic RCS which was verified by comparison with the numerical calculation and full-sized measurements reported in the literature. By measuring and analyzing the variation characteristics of dynamic RCS with frequency, azimuth, and rotational speed, the acquired dynamic RCS was able to be transformed in engineering practice, and it could be considered as data support for solving the reradiation interference of wind turbine to radar station.

2. Wind turbine interference to radar station and its evaluation parameter

2.1. Theory of reradiation interference

When the radar detects the surrounding targets, the antenna will emit electromagnetic waves within a certain range of angles. Wind turbine as an electrically large size target, when electromagnetic wave irradiates it, it will generate induced current on wind turbine, which in turn radiates electromagnetic wave outwards, making the space electromagnetic environment complex. Therefore, the working performance of the radar station was affected seriously [12–14]. This formed the reradiation interference of wind turbine to radar station.

In particular, as the capacity of the wind turbine increases significantly, the blade size, tower height, and cabin length of wind turbine also increase, which leads reradiation interference of wind turbine to radar station to become increasingly prominent.

2.2. Evaluation parameter of reradiation interference

According to the radar principle, the most intuitive description parameter for radar performance is the target echo power received by radar:

$$P_r = P_t \cdot G_t \cdot \frac{1}{4\pi R^2} \cdot \sigma \cdot \frac{1}{4\pi R^2} \cdot \frac{\lambda^2 G_r}{4\pi} \cdot \frac{1}{L} \tag{1}$$

Here P_r is the echo power received by radar, P_t is the transmitting power, G_t is the transmitting antenna gain, G_r is the receiving antenna gain, R is the distance from radar to target, σ is the radar cross-section of the target, λ is the wavelength of the electromagnetic wave, L is the coefficient of the system propagation loss.

Equation (1) is the basic radar equation, which reflects the relationship between the radar detection range and the factors such as the transmitting antenna, the receiving antenna, and the target RCS. It can be seen from Equation (1) that the parameter that change with the change of the target is σ, and the others are the fixed parameters of the radar system. Therefore, current researches use wind turbine RCS parameter to evaluate the reradiation interference level of wind turbine to radar station.

According to the above analysis, the reradiation interference of wind turbine to radar station is actually the electromagnetic scattering problem of wind turbine after being irradiated by external electromagnetic wave. However, due to the blade rotation, the electromagnetic scattering characteristic exhibited by wind turbine is quite different from those of general stationary targets, which is represented by a set of dynamic RCS time series with Doppler characteristic. Therefore, the key to solving the reradiation interference of wind turbine to radar station is to acquire accurate dynamic RCS.

2.3. Theory of numerical calculation of dynamic RCS and its existing problems

At present, the researches on the numerical calculation of wind turbine dynamic RCS are based on the idea of quasistatic. This method requires accurate modeling of the running attitude of the wind turbine at each moment. Furthermore, a high-frequency approximation algorithm such as physical optics (PO) is used to solve the blade RCS at each moment. Finally, the dynamic RCS of the wind turbine is acquired [5].

If the numerical calculation method is used to solve the wind turbine dynamic RCS, the calculation amount and complexity are too large to be accepted. Experimental measurement of the wind turbine scaling model will avoid these problems.

The position diagram of radar and wind turbine is shown in Figure 1. When the radar is working, electromagnetic waves of different frequencies are emitted from different directions, and the rotational speed of the wind turbine blade also changes according to changes in wind direction and wind speed. These factors all affect the wind turbine dynamic RCS. Therefore, when performing the dynamic RCS experimental measurement of wind turbine scaled model, the control variable method is adopted, wind turbine dynamic RCS at different frequencies, azimuths, and rotational speeds are measured.

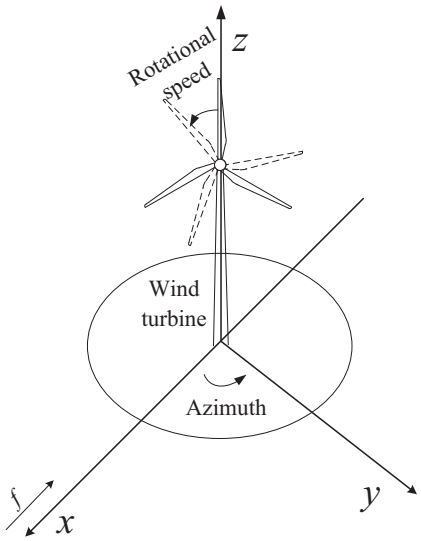

Figure 1. The position diagram of radar and wind turbine.

3. Experimental measurement

3.1. Theory of experimental measurement on scaled model

The scattering field in both full-size space and scaled-size space must satisfy the Maxwell equations:

$$\nabla \times \boldsymbol{E} = -\mu \frac{\partial \boldsymbol{H}}{\partial t}, \tag{2}$$

$$\nabla \times \boldsymbol{H} = \varepsilon \frac{\partial \boldsymbol{E}}{\partial t} + \sigma \boldsymbol{E}, \tag{3}$$

where $\boldsymbol{E}$ and $\boldsymbol{H}$ are the electromagnetic field vectors; σ, μ, and ε are electrical conductivity, permeability, and dielectric constant, respectively; t is time.

Assume the electromagnetic field parameters in the two spaces are as follows:

$$\boldsymbol{E}_1 = k_E \boldsymbol{E}_2, \tag{4}$$

$$\boldsymbol{H}_1 = k_H \boldsymbol{H}_2, \tag{5}$$

$$d_1 = k d_2, \tag{6}$$

$$f_1 = k_f f_2, \tag{7}$$

$$\sigma_1 = k_\sigma \sigma_2, \tag{8}$$

$$\mu_1 = k_\mu \mu_2, \tag{9}$$

$$\varepsilon_1 = k_\varepsilon \varepsilon_2, \tag{10}$$

where $\boldsymbol{E}_1$, $\boldsymbol{H}_1$, d_1, f_1, σ_1, μ_1, and ε_1 are the scaled-size space parameters; $\boldsymbol{E}_2$, $\boldsymbol{H}_2$, d_2, f_2, σ_2, μ_2, and ε_2 are the full-size space parameters; k_E, k_H, k, k_f, k_σ, k_μ and k_ε are the corresponding scale factors. Substituting equation (4) - (10) into equation (2) and (3), then if the scattering fields of the two spaces are accurately approximated, there must be:

$$\frac{k k_\sigma k_E}{k_H} = \frac{k k_f k_\varepsilon k_E}{k_H} = \frac{k k_f k_\mu k_H}{k_E} = 1. \tag{11}$$

Since the medium of the two spaces in measurement environment are ordinary air, the wave impedance of the test medium is constant, that is, $\boldsymbol{E}_1/\boldsymbol{H}_1 = \boldsymbol{E}_2/\boldsymbol{H}_2$, and $k_H = k_E$. In addition, the dielectric constants of the two spaces are the same under ideal test conditions, namely $k_\mu = k_\varepsilon$, then equation (11) can be converted into:

$$k_\sigma = k_f = \frac{1}{k}. \tag{12}$$

On the other hand, wind turbine blades are normally made of nonmagnetic resin materials that have extremely small electrical conductivity. Therefore, the influence of conductivity on the experiment can be neglected, and only the conversion of the electromagnetic wave emission frequency is considered.

3.2. Procedure of the experimental measurement

The size parameter of a full-size model of $Jinfeng77/1500$ wind turbine is shown in Figure 2a. Considering the limits of the frequency band in the measurement, the fidelity of the scaled model etc., the scale factor k was determined to be $1:60$, and the scaled model is shown in Figure 2b. The equipment and parameters used for the experiment are shown in Table 1.

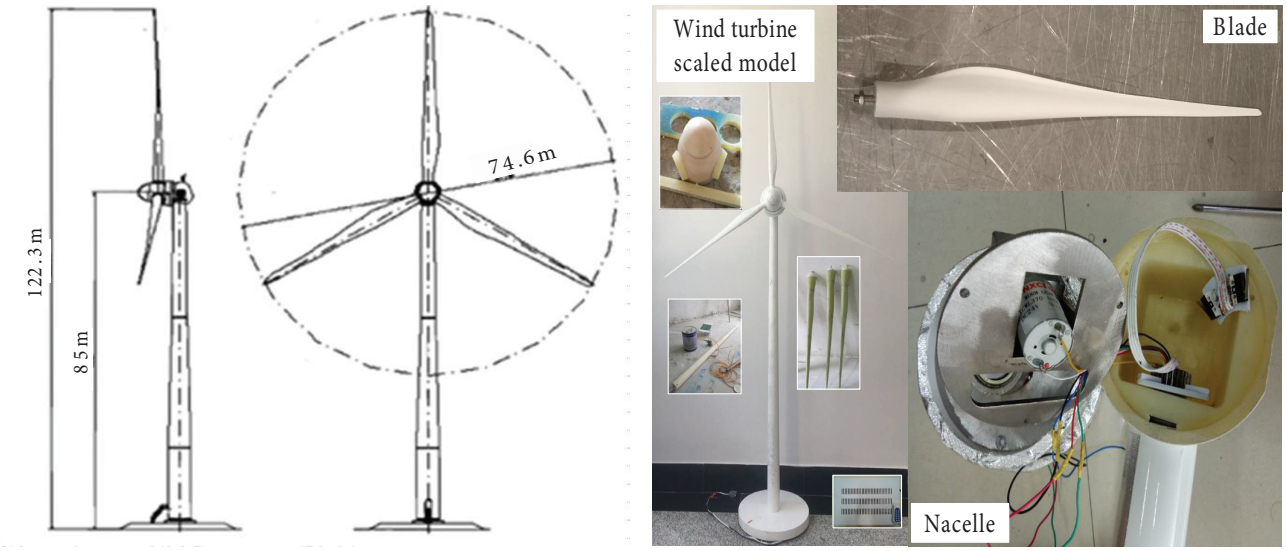

(a) The parameters offull-size model diagram

(b) The production details of scaled model

Figure 2. The parameters of full-size model and the production of scaled model.

Table 1. Experimental equipment and related parameters.

Equipment	Parameter	Remark
Vector network analyzer	Type: $AV3672C-S$	Signal transmission and reception
Antenna 1	Type: $SAS-571$	Signal transmission
Antenna 2	Type:$AT4418$	Signal reception
Microwave cables 1	Length: 10 m	Vector network analyzer to transmitting antenna
Microwave cables 2	Length: 5 m	Vector network analyzer to receiving antenna
Standard ball	Diameter: 500 mm	Determine the target
Anechoic chamber	Size: 35 m $\times$ 25 m $\times$ 15 m	Semianechoic SAR absorber

The procedure of the experimental measurement is as follows:

Step 1: Experimental platform establishing. It is necessary for this platform to ensure the scaled model lying in the far field, so the distance between the scaled model and the antenna was determined to be 3.5 m by simplified calculation.

Step 2: Equipment checking. The main object needs to be checked is the microwave cable. By setting up the short circuit connection of the microwave cable on the vector network analyzer, the status of microwave cable was judged by whether the cable had leakage.

Step 3: Experimental parameters setting. This mainly includes electromagnetic wave transmitting frequency and polarization mode, sampling points and sampling frequency.

Step 4: Measurement and data storage. Since a clicker controlled the blade, we started to measure and save relevant data after the blade rotation was stable.

The experimental arrangement and measurement site of the anechoic chamber are shown in Figure 3.

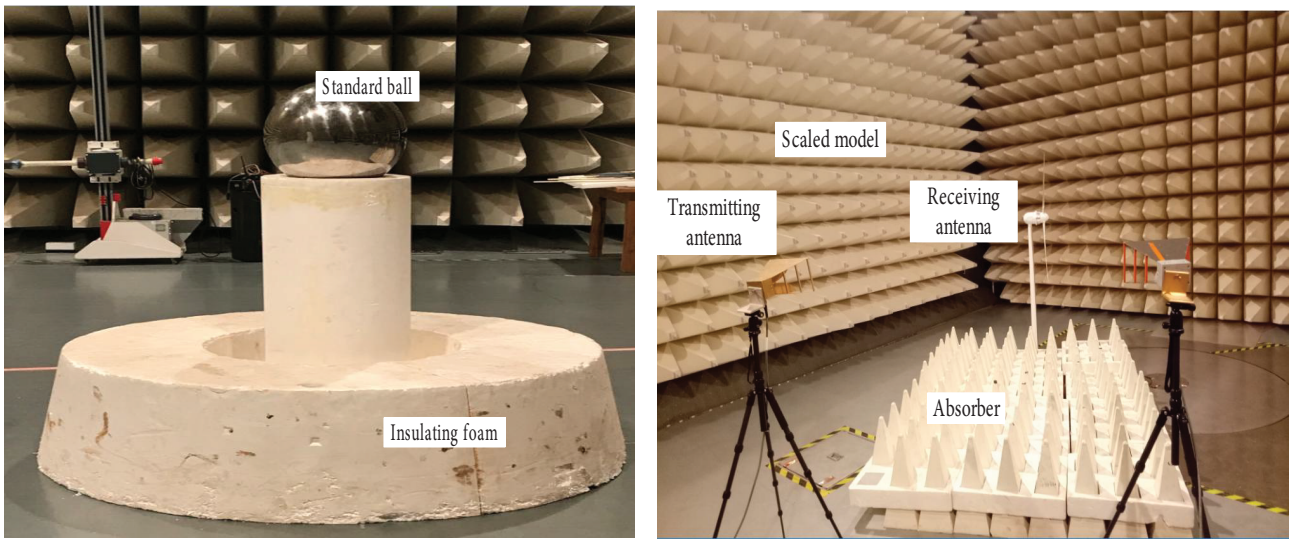

(a) Standard ball used in the calibration process

(b) The experimental arrangement

Figure 3. Experimental site.

The specific measure process of wind turbine dynamic RCS is as follows. Firstly, the results should be calibrated; measure the RCS value of the standard ball of known RCS, as shown in Figure 3a, and compare the two values, if the same, the calibration is successful; then replace the standard ball with the scaled model, as shown in Figure 3b; then, measure the RCS of the scaled model. Finally, according to Equation (13), the RCS of scaled model can be obtained.

$$\sigma(t) = \sigma_2(t) - (\sigma_1(t) - \sigma_0(t)), \tag{13}$$

where $\sigma(t)$ is the RCS data of the scaled model; $\sigma_1(t)$ is the measurement data of the standard ball in the environment during the calibration process, $\sigma_2(t)$ is the measurement data of the wind turbine scaled model, $\sigma_0(t)$ is the RCS value of the standard ball. In our experiments, the standard ball was 250 mm in radius, and its RCS $\sigma_0(t)$ was -7.0 dBsm; it did not change with time.

3.3. Verification of the experimental result

The same geometry model is established by using of FEKO electromagnetic calculation software. The high-frequency approximation algorithm is used to calculate the RCS of this model, and the variation law of RCS data curve is analyzed to verify the validity of the experimental measurement results. Since FEKO cannot achieve electromagnetic scattering calculation of dynamic target, in order to simulate the dynamic rotation characteristics of wind turbine, the idea of quasistatic is adopted. The effect of the rotational motion is achieved by changing the position of the excitation. The idea of quasistatic for solving dynamic RCS of wind turbine requires very strict azimuth angle, and only when azimuth angle $\alpha = 90°$ can accurately simulate this rotational motion. Therefore, when the azimuth angle $\alpha = 90°$, we calculate the dynamic RCS of wind turbine to verify the accuracy of the experimental measurement.

It should be noted that in the process of model establishment, a glass-fiber-reinforced plastic, whose ε is 4.0, is used. In the simulation calculation, the blade rotation speed can be adjusted by controlling the simulation step size and the pulse repetition frequency. The comparison between experimental measurement and simulation calculation at a frequency of 10 GHz, an azimuth angle of $\alpha = 90°$, and a rotational speed of 0.435 r/s is shown in Figure 4a.

We compared the experimental result with the calculation and the full-size wind turbine measurement result reported by Kent et al. in [7] as shown in Figure 4b, to see the validity of the experimental results.

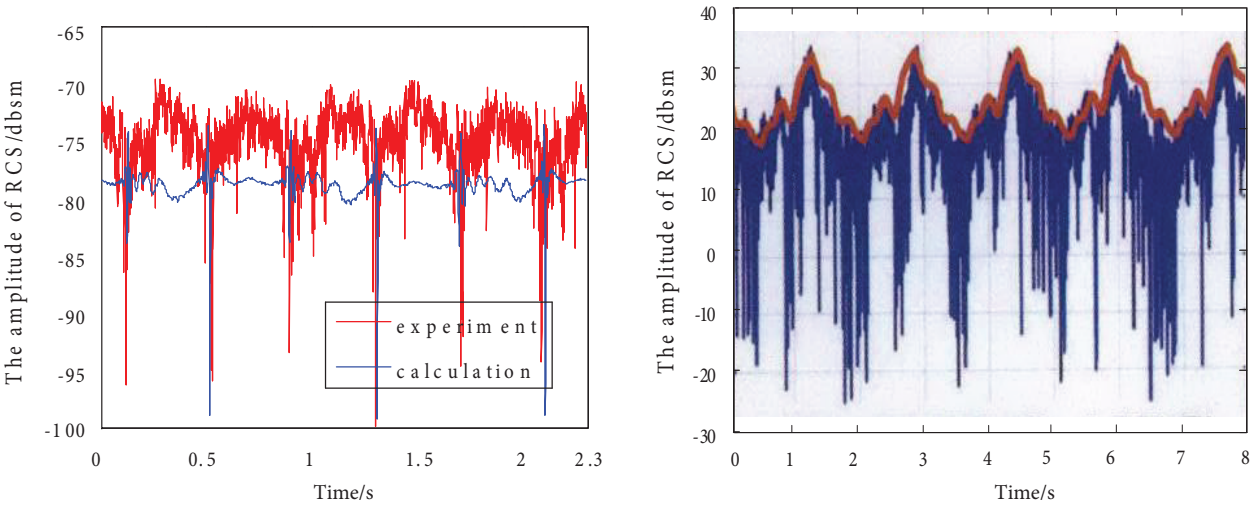

(a) Results of experimental and simulation

(b) The full-size wind turbine measurement result

Figure 4. Comparison diagram of experimental result and calculation result.

As can be seen from Figure 4a, due to the approximation of PO algorithm, the scattering of electromagnetic waves on the wind turbine was different from those of the practical situation, which makes the peaks of RCS inconsistent and the maximum and minimum values of RCS appear at the same time. The full-size wind turbine measurement results shown in Figure 4b can completely illustrate these differences. In addition, the time intervals between the peaks are the same. This shows that the Doppler effect exhibited by the dynamic RCS are similar, which is an important reason why the numerical calculation method could be used to qualitatively analyze the dynamic RCS of wind turbines.

It is worth noting that we use the glass fiber reinforced plastic to build the scaled model to acquire the actual electromagnetic scattering of the wind turbine. Nevertheless, in actual engineering, in order to protect the wind turbine from lightning, the steel wires are covered on the surface, which will enhance its electrical conductivity and make the amplitude of RCS larger. This is the main reason for the error in our experimental results.

4. Measurement results and analysis

Dynamic RCS of wind turbine is different from the RCS of stationary targets. It is related not only to the frequency and direction of the electromagnetic wave emitted by the radar, but also to the rotational speed of the blades. Therefore, in order to analyze the characteristics of dynamic RCS of wind turbine, our experiment used control variables method and considered parameters including the frequency, azimuth, and the rotational speed of the blade.

4.1. Influence of frequency on dynamic RCS

The measurements were performed with azimuth $\alpha = 0°$, rotational speed of blade 0.435 r/s, and electromagnetic wave emission frequencies of 5 GHz, 10 GHz, and 15 GHz. The amplitude and phase data of measured dynamic RCS are shown in Figure 5.

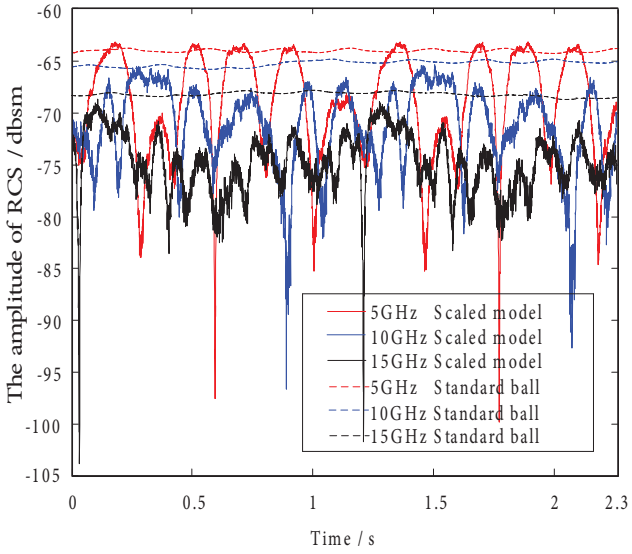

(a) The amplitude of dynamic RCS

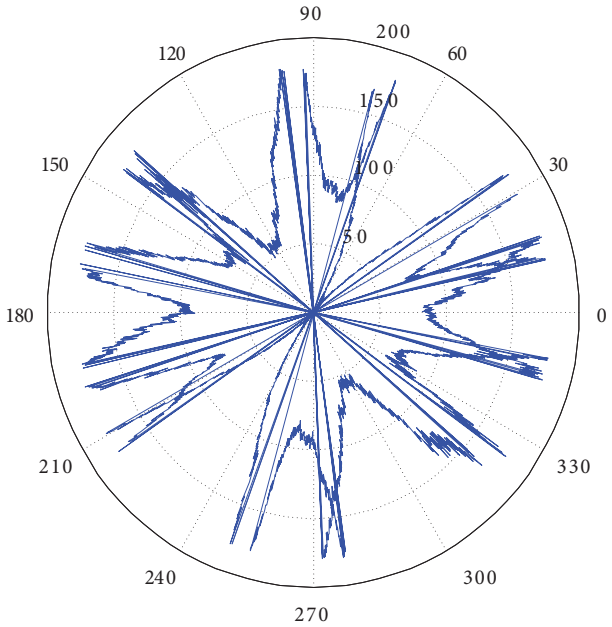

(b) The phase of RCS at 10GHz frequency

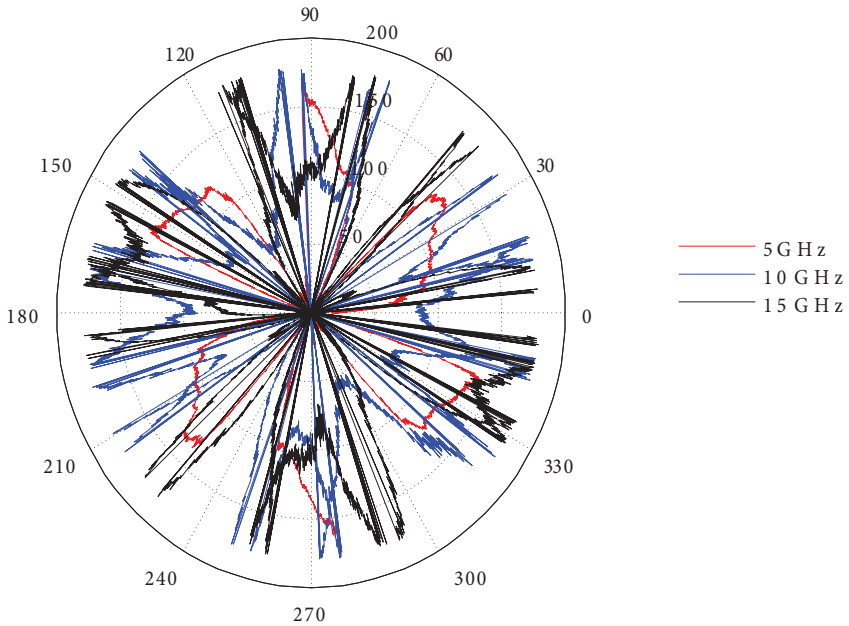

(c) The phase of RCS at various frequencies

Figure 5. Influence of frequency on dynamic RCS.

As shown in Figure 5a, it is easy to tell that the RCS peaks show a trend of decreasing with increasing frequency. Considering the theory of scaled model and using Equation (13), we calculated the maximum values of RCS for the wind turbine of the $Jinfeng77/1500$ at 83.3 MHz, 166.6 MHz, and 250.0 MHz in actual engineering, which would be 29.43 dbsm, 28.69 dbsm, and 28.21 dbsm, respectively. These rather big values show an important reason why wind turbines are often used as the size of electric power structures in the research field of electromagnetic scattering.

The Doppler effect exhibited by the RCS phase curve is more obvious during a rotation cycle, as shown in Figures 5b and 5c, among them, Figure 5b is phase curve at 10 GHz frequency, Figure 5c is the phase curves at various frequencies. It is easy to see that there are 6 peaks in the RCS phase; starting at 30°, a peak occurs every 60°, which indicates that the scattering intensity of different blade positions are different during the rotation of wind turbine blade.

4.2. Influence of azimuth on dynamic RCS

The influence of azimuth on dynamic RCS are shown in Figure 6. The measurements were performed with blade rotation speed of 0.435 r/s, frequency of 10 GHz, and azimuth of 0°, 45°, and 90°.

As shown in Figure 6a, the wind turbine RCS is maximal when the electromagnetic wave is perpendicular to the plane of wind turbine blade, that is, azimuth $\alpha = 0^\circ$. This is because when α is 0°, the wind turbine blade provides specular reflection, so the RCS is the largest and the occlusion effect is also the most serious. When α is 90°, the wind turbine blade provides edge diffraction, so the RCS is small, and the corresponding occlusion influence is also slightly reduced. The maximum difference between the two RCS amplitudes is 4.102 dbsm.

The phase curve are shown in Figures 6b and 6c, among them, Figure 6b is phase curve at 0° azimuth, Figure 6c is the phase curves at various azimuths. The phase peak of RCS exhibits a band shape when the azimuth α is 0°, which indicates that the wind turbine blade has large scattering intensity at a certain stance and the vicinity of this stances. When the azimuth α is 90°, the RCS phase peak exhibits a spike shape, which indicates that the stances of the wind turbine provide instantaneous maximum scattering intensity. This is obviously different from the conclusions obtained by the traditional numerical calculation method of wind turbine scattering point superposition model [15]. This simplified wind turbine model equivalents a wind turbine into a series of linear discrete scattering points; using it comes to a conclusion that when the azimuth α is 0°, the distance between the scattering point of the wind turbine blade and the radar does not change, that is, the blade rotation does not affect the electromagnetic wave modulation. The difference between the experimental results in this paper and the simplified numerical model comes mainly because the scattering point superposition model ignores the irregular curved surface shape of the blade and considers that the scattering intensity of each scattering point is the same. Therefore, the simplified model is generally only used to qualitatively analyze the scattering characteristics of wind turbines.

4.3. Influence of rotational speed on dynamic RCS

For rotational speed, the measurements are performed with frequency of 10 GHz, azimuth α of 90°, and blade rotation speeds of 0.435 r/s and 0.250 r/s.

As shown in Figure 7a, when the frequency and azimuth angle are fixed, the rotational speed barely influences the amplitude of RCS, instead it changes the moment when the peaks occur obviously. The speed of wind turbine blades can be estimated from the time interval between two adjacent peaks in the amplitude

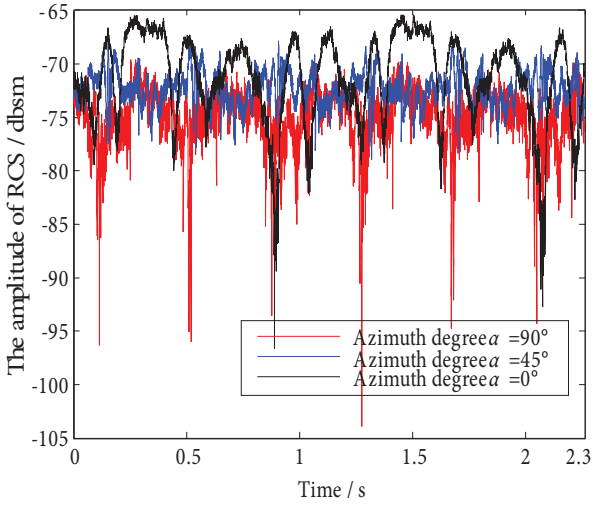

(a) The amplitude of dynamic RCS

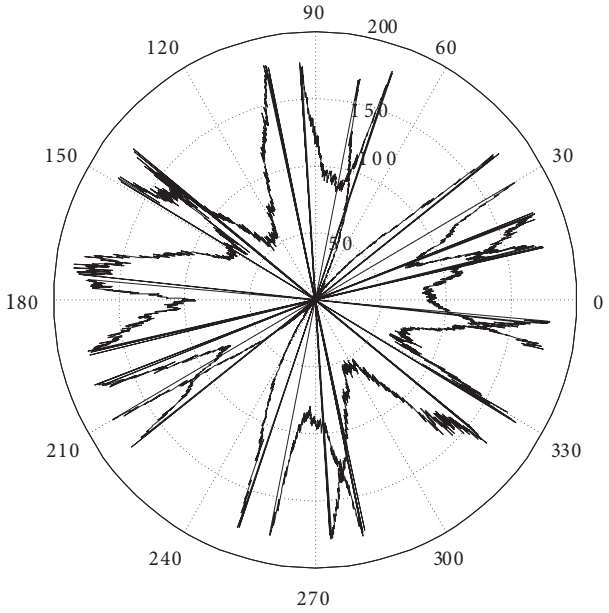

(b) The phase of RCS at 0° azimuth

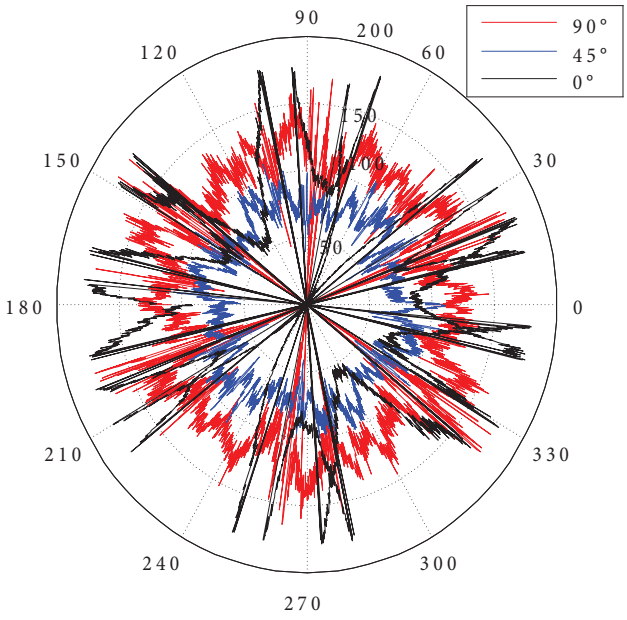

(c) The phase of RCS at various azimuths

Figure 6. Influence of azimuth on dynamic RCS.

curve of dynamic RCS. It is not difficult to find that in the red curve and the blue curve, the two adjacent peak time intervals are 0.67 s and 0.38 s, respectively. Considering the strict symmetry of the blades, this is the time required for the blade to rotate by 60°, from which the corresponding blade speed can be derived.

The RCS phase data is transformed into the variation with blade attitude as shown in Figures 7b and 7c, among them, Figure 7b is phase curve at 0.435 r/s, Figure 7c is the phase curves at various rotational speeds.

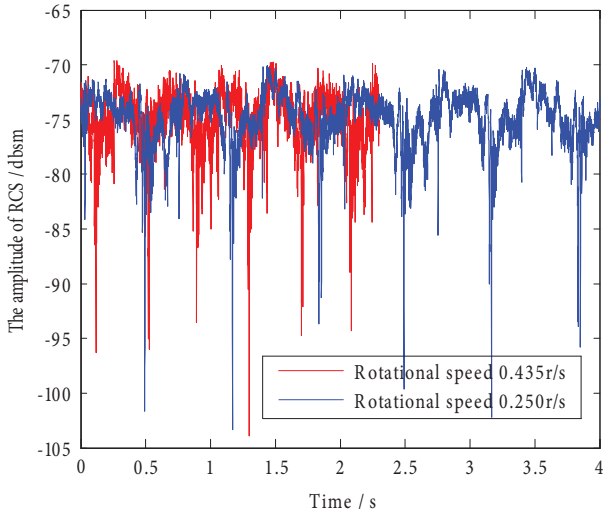

(a) The amplitude of dynamic RCS

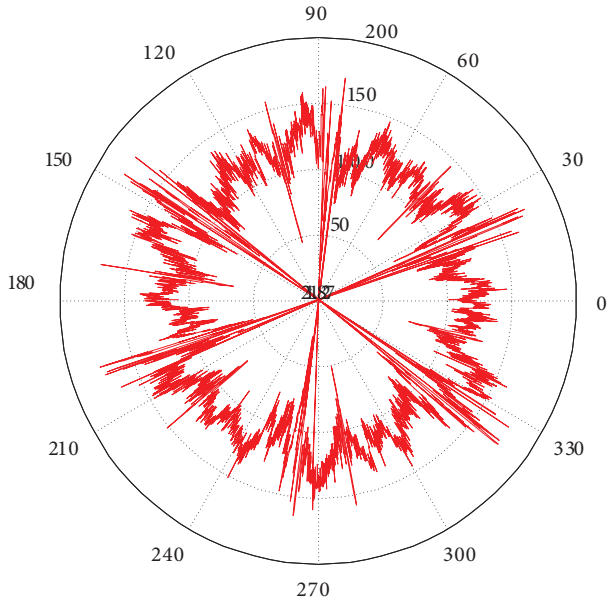

(b) The phase of RCS at 0.435r/s

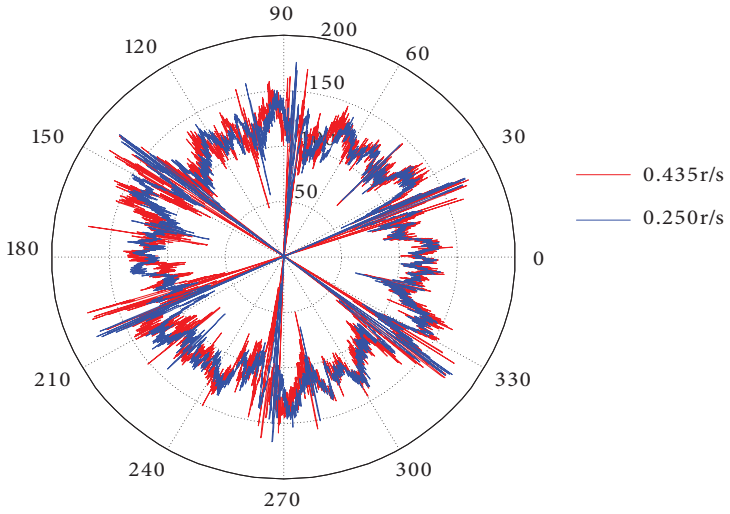

(c) The phase of RCS at various speeds

Figure 7. Influence of rotational speed on dynamic RCS.

The RCS phase peaks appear at the same time, which indicates that the wind turbine blades will have RCS phase peaks in a unique attitude. Combined with the initial analysis of the experimental measurement process, it is concluded that under the condition of azimuth angle of 90°, the RCS phase peak appears when the wind turbine blade is perpendicular to the direction of electromagnetic wave emitted by radar, which is consistent with the conclusion obtained by the numerical calculation method.

5. Conclusion

(1) Using the proposed experimental measurement platform, we were able to measure the dynamic RCS of wind turbine scaled model accurately. The obtained data can be used in quantitative analysis of Doppler effect in

subsequent research.

(2) The dynamic RCS value of the wind turbine is negatively correlated with frequency and azimuth. Among of them, the maximum RCS value can reach up to 29.43 dbsm when the frequency is 83.3 MHz, and the Doppler effect still exists while the azimuth is $0°$.

(3) The rotational speed of blades affects the Doppler effect, which is reflected by the moments of peaks, but does not affect the value of dynamic RCS. When the blade is also perpendicular to the radar line of sight, there would be peaks of dynamic RCS.

Acknowledgment

This work was supported in part by the National Natural Science Foundation of China under Grant 51977121, in part by State Key Laboratory of Power Grid Environmental Protection ($GYW51201901075$).

Contributions of authors

BO TANG gave the experimental program and the idea, HAO CHEN did the experiments and wrote this paper, LI HUANG and FATING YUAN guided the experiments, and FENG PENG recorded experimental data.

References

[1] Karabayir O, Yucedag SM, Coskun AF, Yucedag OM, Serim HA et al. Wind turbine signal modelling approach for pulse Doppler radars and applications. IET Radar, Sonar and Navigation 2015; 9(3): 276-284. doi: 0.1049/iet-rsn.2014.0094

[2] Krich SI, Montanari M, Amendolare V, Berestesky P. Wind turbine interference mitigation using a waveform diversity radar. IEEE Transactions on Aerospace and Electronic Systems 2017; 53(2): 805-815. doi: 10.1109/TAES.2017.2665143

[3] Wu RB, Mao J, Wang XL, Jia QQ. Target detection of primary surveillance radar in wind farm clutter. Journal of Electronics and Information Technology 2013; 35(3): 754-758 (in Chinese). doi: 10.3724/SP.J.1146.2012.00923

[4] Angulo I, Grande O, Jenn D, Guerra D, Vega D. Estimating reflectivity values from wind turbines for analyzing the potential impact on weather radar services. Atmospheric Measurement Techniques Discussions 2015; 8(2): 1477-1509. doi: 10.5194/amt-8-2183-2015

[5] Tang B, Liu R, Zhang JG, Liu XF, Sun R et al. Doppler characteristics of wind turbine blades based on dynamic RCS. High Voltage Engineering 2017; 43(10): 3435-3442 (in Chinese). doi: 10.13336/j.1003-6520.hve.20170925035

[6] Danoon LR, Brown AK. Modeling methodology for computing the radar cross section and doppler signature of wind farms. IEEE Transactions on Antennas and Propagation 2013; 61(10): 5166-5174. doi: 10.1109/TAP.2013.2272454

[7] Kent BM, Hil KC, Butebaugh A, Zelinski G, Hawley R et al. Dynamic radar cross section and radar doppler measurements of commercial general electric windmill power turbines part 1: Predicted and measured radar signatures. IEEE Antennas and Propagation Magazine 2008; 50(2): 211-219. doi: 10.1109/MAP.2008.4562424

[8] Bornkessel C, Schulze S, Hein MA. Measured impact of electromagnetic scattering off wind turbines on broadcast signal propagation. In: IEEE 2016 German Microwave Conference; Bochum, Germany; 2016. pp. 425-428. doi: 10.1109/GEMIC.2016.7461646

[9] Ballesteros MC, Antoniou M, Cherniakov M. Wind turbine blade radar signatures in the near field: Modeling and Experimental Confirmation. IEEE Transactions on Aerospace and Electronic Systems 2017; 53(4): 1916-1931. doi: 10.1109/TAES.2017.2675241

[10] La TV, Pennec FL, Comblet F, Elenga S. 3.5 kW wind turbine for cellular base station: Radar cross section modelling and measurement. In: IEEE 2014 44th European Microwave Conference; Rome, Italy; 2014. pp. 143-146. doi: 10.1109/EuMC.2014.6986390

[11] Zhang Y, Huston A, Palmer RD, Alberston R, Kong FX et al. Using scaled models for wind turbine EM scattering characterization: techniques and experiments. IEEE Transactions on Instrumentation and Measurement 2011; 60(4): 1298-1306. doi: 10.1109/TIM.2010.2085271

[12] Saynak U, Karahan HA, Coskun AF, Yucedag SM, Aldirmaz S et al. Preliminary set of analysis for the assessment of wind turbines which are in the line-of-sight of radar, navigation and communications systems. IET Radar, Sonar and Navigation 2014; 5(8): 415-424. doi: 10.1049/iet-rsn.2013.0228

[13] Nai F, Torres S, Palmer R. On the mitigation of wind turbine clutter for weather radars using range-doppler spectral processing. IET Radar, Sonar and Navigation 2013; 7(2): 178-190. doi: 10.1049/iet-rsn.2012.0225

[14] Li CJ, Bhalla R, Ling H. Investigation of the dynamic radar signatures of a vertical-axis wind turbine. IEEE Antennas and Wireless Propagation Letters 2015; 14: 763-766. doi: 10.1109/LAWP.2014.2377693

[15] He WK, Shi YL, Wang XL, Ma YZ, Wu RB. Simulation and analysis of wind turbine echoes. Journal of System Simulation 2015; 27(1): 50-56 (in Chinese). doi: 10.16182/j.cnki.joss.2015.01.006